INT. J. NUM. METH. HEAT FLUID FLOW, VOL. 6, NO. 8, 3–18 (1996)

THE DEVELOPMENT OF A ONE-STEP ACCURATE FLUX VECTOR-SPLITTING IMPLICIT ALGORITHM FOR EULER AND NAVIER-STOKES EQUATIONS

E.Y.K. NG† AND S.Z. LIU‡

†School of Mechanical and Production Engineering, Nanyang Technological University, Nanyang Avenue, Singapore 639798

‡Gateway Technology Service Pte Ltd, 85 Science Park Drive, Singapore 118230

ABSTRACT

This paper introduces a novel algorithm for solving the two-dimensional Euler and Navier-Stokes compressible equations using a one-step effective flux vector-splitting implicit method. The new approach makes a contribution by deriving a simple and yet effective implicit scheme which has the features of an exact factorization and avoids the solving of block-diagonal system of equations. This results in a significant improvement in computational efficiency as compared to the standard Beam-Warming and Steger implicit factored schemes. The current work has advantageous characteristics in the creation of higher order numerical implicit terms. The scheme is stable if we could select the correct values of the scalars ($\lambda^{\pm}_{\xi}$ and $\lambda^{\pm}_{\eta}$) for the respective split flux-vectors ($F^{\pm}$ and $G^{\pm}$) along the ξ- and η-directions. A simple solving procedure is suggested with the discussion of the implicit boundary conditions, stability analysis, time-step length and convergence criteria. This method is spatially second-order accurate, fully conservative and implemented with general co-ordinate transformations for treating complex geometries. Also, the scheme shows a good convergence rate and acceptable accuracy in capturing the shock waves. Results calculated from the program developed include transonic flows through convergence-divergence nozzle and turbine cascade. Comparisons with other well-documented experimental data are presented and their agreements are very promising. The extension of the algorithm to 3D simulation is straightforward and under way.

KEY WORDS Improved flux splitting No artificial dissipation Internal flow

INTRODUCTION

An implicit scheme which determines the unknowns at each new time-level through the solution of linear algebra systems to avoid the CFL limitation for stability along the time direction, has been implemented widely, especially in solving the Navier-Stokes equations for improving its convergent rate and computational efficiency. The development of an implicit scheme is classified into two approaches:

(1) the implicit approximate factorization (AF) method such as the schemes by Beam and Warming[1] and MacCormack[2]. These methods are widely used because they can solve the block-tridiagonal (or block-bidiagonal) algebra equations at each dimension, with less computational efforts. The scheme has been modified and improved by Von Lavante and Lyer[3], Dawes[4] and Jameson[5]. They used the spectral radii technique instead of the matrix calculation. The common characteristic of these methods are that they stress the simplifying of implicit algebraic equations and enable the higher dimension problems to reduce to the lower dimension one. However, the use of approximate factorization will inevitably increase the truncation error with a large time step. Thus the precision and stability of the scheme are affected, and this can cause an unstable situation when it is applied to the 3D problem.

0961–5539/96

Received September 1995
Revised March 1996

(2) the method without any approximate factorization but to solve the five diagonal (2D) or seven diagonal (3D) matrix equations directly by using some effective algebra methods, such as the strongly implicit procedure by Sankar *et al.*[6] and the Guass-Seidel interaction method by Ames[7]. The method has good compatibility where higher CFL numbers can be used; however, its drawback is that a greater amount of computational effort is required.

Combining the advantages of the above two approaches (i.e. by using the spectral radii technique to simplify the calculation and by avoiding the approximate factorization to increase the CFL number and stability), we may obtain an improved implicit scheme which has the characteristics of exact factorization and avoiding the solving of the block-diagonal system of equations. Thus, the objective of the present work is to develop a simple and yet efficient flux vector-splitting implicit scheme which possesses the above characteristics. The first-order implicit scheme for Euler equations is developed initially and then extended to the second-order accuracy for Navier-Stokes equations. A simple solving method is also suggested with the discussion of the implicit boundary conditions, stability analysis, time-step length and convergence criteria. Finally, an investigation of the various aspects of the algorithm against flows with reliable experimental data are included.

MATHEMATICAL MODEL

The governing equations in body-fitted co-ordinate system

The 2D transformed Navier-Stokes (1) and Euler equations (2) are written as (see Anderson *et al.*[8]):

$$\frac{\partial \hat{U}}{\partial t}+\frac{\partial \hat{F}}{\partial \xi}+\frac{\partial \hat{G}}{\partial \eta}=\frac{1}{\mathrm{Re}}\left(\frac{\partial \hat{Q}}{\partial \xi}+\frac{\partial \hat{R}}{\partial \eta}\right) \tag{1}$$

and

$$\frac{\partial \hat{U}}{\partial t}+\frac{\partial \hat{F}}{\partial \xi}+\frac{\partial \hat{G}}{\partial \eta}=0 \tag{2}$$

where $\hat{U}=\frac{1}{J}\begin{bmatrix}\rho\\ \rho u_x\\ \rho u_y\\ E\end{bmatrix}$, $\hat{F}=\frac{1}{J}\begin{bmatrix}\rho\tilde{u}_x\\ \rho u_x\tilde{u}+P\xi_x\\ \rho u_x\tilde{u}+P\xi_y\\ (E+P)\tilde{u}\end{bmatrix}$, $\hat{G}=\frac{1}{J}\begin{bmatrix}\rho\tilde{v}\\ \rho u_x\tilde{v}+P\eta_x\\ \rho u_y\tilde{v}+P\eta_y\\ (E+P)\tilde{v}\end{bmatrix}$,

$\hat{Q}=\frac{1}{J}\begin{bmatrix}0\\ \tau_{xx}\xi_x+\tau_{xy}\xi_y\\ \tau_{xy}\xi_x+\tau_{yy}\xi_y\\ \beta_x\xi_x+\beta_y\xi_y\end{bmatrix}$, $\hat{R}=\frac{1}{J}\begin{bmatrix}0\\ \tau_{xx}\eta_x+\tau_{xy}\eta_y\\ \tau_{xy}\eta_x+\tau_{yy}\eta_y\\ \beta_x\eta_x+\beta_y\eta_y\end{bmatrix}$ and

$\left.\begin{aligned}\tilde{u}&=u\xi_x+v\xi_y\\ \tilde{v}&=u\eta_x+v\eta_y\end{aligned}\right\}$ are the contravariant along ξ and η coordinates respectively.

Explicit boundary conditions

The solution at the farfield boundaries is not known a priori since it is affected by the flow within the computational domain. Thus, boundary conditions must evolve with calculation. Ideally, these boundary conditions should be treated as a physically relevant solution and do not cause non-physical reflection of waves passing through the domain. Hedstrom[9] has shown that this can be done by performing a characteristic analysis of the 1D equations normal to the boundaries. The number and type of conditions specified are determined by those characteristics that enter the domain. At the inlet, the right-moving characteristics enter the domain. Thus, four boundary conditions are specified for supersonic inflow, and three are specified for subsonic inflow.

Obviously, the solid boundary conditions for viscous flow is a no-slip condition. In addition, the solid wall pressure and density conditions: $\left.\frac{\partial P}{\partial n}\right|_w = 0$ and $\left.\frac{\partial \rho}{\partial n}\right|_w = 0$ are used to determine these parameters. However, in the case of inviscid flow, it is necessary to satisfy the slip condition. This is expressed by the vanishing of the normal velocity $v_n = 0$.

NUMERICAL DISCRETIZATION

The analysis of implicit scheme construction

The non-linear flux vectors F and G of equations (1) and (2) are homogeneous functions of degree one. We can split the flux vectors $F^{\pm}$ and $G^{\pm}$ of every computational point into two subvectors respectively according to the positive and negative eigenvalues. The subvectors F^{+} and G^{+}, which have positive eigenvalues, use the backward-difference operator whereas the subvectors F^{-} and G^{-} which have negative eigenvalues which apply the forward-difference operator.

The Euler equations (2) can be rewritten as:

$$\frac{\partial U}{\partial t} + A\frac{\partial F}{\partial \xi} + B\frac{\partial G}{\partial \eta} = 0 \tag{3}$$

where A and B are the Jacobian matrices $\partial F/\partial U$ and $\partial G/\partial U$ respectively. In general, they are homogeneous matrices which exist in a similarity transformation[9] such that:

$$\begin{aligned} Q^{-1}AQ &= \Lambda(A) = diag[\tilde{U},\ \tilde{U},\ \tilde{U} + aL(\xi),\ \tilde{U} - aL(\xi)] \quad \text{and} \\ Q^{-1}BQ &= \Lambda(B) = diag[\tilde{V},\ \tilde{V},\ \tilde{V} + aL(\eta),\ \tilde{V} - aL(\eta)] \end{aligned} \tag{4}$$

where Λ is the diagonal matrix, a is the speed of sound in physical domain, and

$$\tilde{U} = u\frac{\partial \xi}{\partial x} + v\frac{\partial \xi}{\partial y},\ \tilde{V} = u\frac{\partial \eta}{\partial x} + v\frac{\partial \eta}{\partial y}$$

$$L(\xi) = \sqrt{\xi_x^2 + \xi_y^2},\ L(\eta) = \sqrt{\eta_x^2 + \eta_y^2}\ .$$

From equation (4), we have the eigenvalues:

$\lambda_1 = \lambda_2 = \tilde{U}$, $\lambda_3 = \tilde{U} + aL(\xi)$ and $\lambda_4 = \tilde{U} - aL(\xi)$ for flux vector F and

$\lambda_1 = \lambda_2 = \tilde{V}$, $\lambda_3 = \tilde{V} + aL(\eta)$ and $\lambda_4 = \tilde{V} - aL(\eta)$for flux vector G.

Based on these positive and negative eigenvalues, the expressions for calculating the subvectors $F^{\pm}$ and $G^{\pm}$ can be simplified and summarized as follows:

$$F^{\pm}=\frac{J\rho}{2\gamma}\begin{bmatrix} C_1 \\ C_1u+C_2a\bar{\xi}_x \\ C_1v+C_2a\bar{\xi}_y \\ C_1(u^2+v^2)/2+C_2a\bar{\xi}_xu+C_2a\bar{\xi}_yv+C_3a^2/(\gamma-1) \end{bmatrix}$$

$$G^{\pm}=\frac{J\rho}{2\gamma}\begin{bmatrix} C_1 \\ C_1u+C_2a\bar{\eta}_x \\ C_1v+C_2a\bar{\eta}_y \\ C_1(u^2+v^2)/2+C_2a\bar{\eta}_xu+C_2a\bar{\eta}_yv+C_3a^2/(\gamma-1) \end{bmatrix} \tag{5}$$

where $C_1 = 2(\gamma-1)\lambda_1 + \lambda_3 + \lambda_4$, $C_2 = \lambda_3 - \lambda_4$, $C_3 = \lambda_3 + \lambda_4$ and $\bar{\xi}_x = \xi_x/L(\xi), \bar{\xi}_y = \xi_y/L(\xi)$, $\bar{\eta}_x = \eta_x/L(\eta)$, $\bar{\eta}_y = \eta_y/L(\eta)$ are the constants on computational point (i, j). When calculating the F^+ and G^+ terms, the positive eigenvalues are used with any negative eigenvalue set to zero. Conversely, when calculating F^- and G^- terms, the negative eigenvalues are used with the positive one set to zero. The final equations for solving inviscid flow in the flux vector-splitting form are thus:

$$\frac{\partial U}{\partial t}+\frac{\partial F^+}{\partial \xi}+\frac{\partial F^-}{\partial \xi}+\frac{\partial G^+}{\partial \eta}+\frac{\partial G^-}{\partial \eta}=0 \tag{6}$$

For Navier-Stokes equations (1), the RHS terms, i.e. viscous flux-vectors Q and R, mainly consist of the first-order derivative of variables u, v and T. First, the direction of the information dependent region for Navier-Stokes solutions corresponding to Q and R does not change with the velocity, therefore it is not necessary to choose the difference direction according to the eigenvalues. Second, the first-order derivatives $\rho\xi$, $i\xi$, $v\xi$ and $T\xi$ in the Q and R only bring the upward influence for the solution while the second-order derivatives $\rho_{\xi\xi}$, etc. induce both the upward and backward influences for the solution. Therefore flux vectors Q and R should use the two-side differencing and need not be split into the subvectors. The final equations with flux vector-splitting form for viscous flow are therefore obtained accordingly as follows:

$$\frac{\partial U}{\partial t}+\frac{\partial F^+}{\partial \xi}+\frac{\partial F^-}{\partial \xi}+\frac{\partial G^+}{\partial \eta}+\frac{\partial G^-}{\partial \eta}=\frac{1}{\mathrm{Re}}\left(\frac{\partial Q}{\partial \xi}+\frac{\partial R}{\partial \eta}\right) \tag{7}$$

In brief, the problem which exists in all of these schemes is that the approximation factorization techniques are all adopted in their smoothing for implicit calculation. These cause the difficulties in the stability for the 3D calculations.

The construction of an efficient flux vector-splitting implicit scheme

A new implicit numerical scheme can be constructed if its associated smoothing method for implicit simulation has a characteristic of unconditional stability. Using the idea of formulating an implicit scheme without approximate factorization and the coefficient block-diagonal system of equations together with the concept of characteristics for flux vector-splitting, the following higher-order extra small terms

$$-\Delta t\frac{\partial}{\partial\xi}(\lambda_\xi^+\frac{\partial U}{\partial t}),\ \Delta t\frac{\partial}{\partial\xi}(\lambda_\xi^-\frac{\partial U}{\partial t})$$

$$-\Delta t\frac{\partial}{\partial\eta}(\lambda_\eta^+\frac{\partial U}{\partial t}),\ \Delta t\frac{\partial}{\partial\eta}(\lambda_\eta^-\frac{\partial U}{\partial t})$$

can be added to the right-hand side of the equations (6) and (7) directly to form the implicit schemes for the Euler and Navier-Stokes equations respectively. The approximate partial differential equations of (6) and (7) can therefore be obtained as follows:

$$\frac{\partial U}{\partial t}+\frac{\partial F^+}{\partial\xi}+\frac{\partial F^-}{\partial\xi}+\frac{\partial G^+}{\partial\eta}+\frac{\partial G^-}{\partial\eta}=-\Delta t\frac{\partial}{\partial\xi}(\lambda_\xi^+\frac{\partial U}{\partial t})+\Delta t\frac{\partial}{\partial\xi}(\lambda_\xi^-\frac{\partial U}{\partial t})$$
$$-\Delta t\frac{\partial}{\partial\eta}(\lambda_\eta^+\frac{\partial U}{\partial t})+\Delta t\frac{\partial}{\partial\eta}(\lambda_\eta^-\frac{\partial U}{\partial t}) \tag{8}$$

and,

$$\frac{\partial U}{\partial t}+\frac{\partial F^+}{\partial\xi}+\frac{\partial F^-}{\partial\xi}+\frac{\partial G^+}{\partial\eta}+\frac{\partial G^-}{\partial\eta}=\frac{1}{\mathrm{Re}}(\frac{\partial Q}{\partial\xi}+\frac{\partial R}{\partial\eta})\ -\Delta t\frac{\partial}{\partial\xi}(\lambda_\xi^+\frac{\partial U}{\partial t})+\Delta t\frac{\partial}{\partial\xi}(\lambda_\xi^-\frac{\partial U}{\partial t})$$
$$-\Delta t\frac{\partial}{\partial\eta}(\lambda_\eta^+\frac{\partial U}{\partial t})+\Delta t\frac{\partial}{\partial\eta}(\lambda_\eta^-\frac{\partial U}{\partial t}) \tag{9}$$

In equations (8) and (9), the higher-order extra terms

$$-\Delta t\frac{\partial}{\partial\xi}(\lambda_\xi^+\frac{\partial U}{\partial t}),\ \Delta t\frac{\partial}{\partial\xi}(\lambda_\xi^-\frac{\partial U}{\partial t})$$

are the implicit construction items for the convection fluxes $F\pm$ respectively along the ξ direction, where $\lambda_\xi^\pm$ are the scalars corresponding to the eigenvalues of the matrices $F^\pm$. Likewise,

$$-\Delta t\frac{\partial}{\partial\xi}(\lambda_\xi^+\frac{\partial U}{\partial t}),\ \Delta t\frac{\partial}{\partial\xi}(\lambda_\xi^-\frac{\partial U}{\partial t})$$

are the implicit construction items for the fluxes $G^\pm$ respectively along the η direction, where $\lambda_\eta^\pm$ are the scalars corresponding to the eigenvalues of matrices $G^\pm$. This newly formed implicit scheme is stable if we could select the correct values for the scalars (i.e. $\lambda_\xi^\pm$ and $\lambda_\eta^\pm$).

Notice that the newly added terms are the unsteady items corresponding to the $\partial U/\partial t$, therefore, we can say that as far as the theory is concerned, they have no influence on the solution once it has converged to the steady state.

By differencing equation (8) and rearranging, we obtain:

$$\Delta U_{i,j}^n=-\Delta t[\frac{\nabla_x F^+}{\Delta\xi}+\frac{\Delta_x F^-}{\Delta\xi}+\frac{\nabla_x G^+}{\Delta\eta}+\frac{\Delta_x G^-}{\Delta\eta}] \tag{10-1}$$

$$(1+\lambda_\xi^+\frac{\Delta t}{\Delta\xi}+\lambda_\xi^-\frac{\Delta t}{\Delta\xi}+\lambda_\eta^+\frac{\Delta t}{\Delta\eta}+\lambda_\eta^-\frac{\Delta t}{\Delta\eta})\delta U_{i,j}^{n+1}=\Delta U_{i,j}^{n}+\frac{\Delta t}{\Delta\xi}\lambda_\xi^+\delta U_{i-1,j}^{n+1}+\frac{\Delta t}{\Delta\xi}\lambda_\xi^-\delta U_{i+1,j}^{n+1}$$
$$+\frac{\Delta t}{\Delta\eta}\lambda_\eta^+\delta U_{i,j-1}^{n+1}+\frac{\Delta t}{\Delta\eta}\lambda_\xi^-\delta U_{i,j+1}^{n+1} \qquad (10\text{-}2)$$

Now, equation (10-1) can be considered as an explicit step that describes the physical conservation law while equation (10-2) can be considered as an implicit step to ensure the calculation stability for a large time step. For inviscid flow, the explicit step $\Delta U_{i,j}^{n}$ can be differenced with either first-order accuracy by using two-point backward and forward methods or second-order accuracy by using three-point backward and forward methods. In scheme (10), as the terms $\lambda_\xi^{\pm}$ and $\lambda_\eta^{\pm}$ are all scalars, thus the computational efforts are reduced greatly as compared to the other coefficient matrix implicit schemes for all time steps n, such as those by Chakravarthy *et al.*[10] and Moretti[11]. The major characteristic of the present scheme is that of exact factorization approach. Furthermore, the above scheme is a one-step method which has the added advantage for calculation with a large timestep where the same difference scheme should be used to obtain the convergent solution without oscillations.

Similarly, we could obtain the difference scheme for Navier-Stokes equations (9) as follows:

$$\Delta U_{i,j}^{n}=-\Delta t[\frac{\nabla_x F^+}{\Delta\xi}+\frac{\Delta_x F^-}{\Delta\xi}+\frac{\nabla_x G^+}{\Delta\eta}+\frac{\Delta_x G^-}{\Delta\eta}]+\frac{1}{\mathrm{Re}}(\frac{DQ}{\Delta\xi}+\frac{DR}{\Delta\eta}) \qquad (11\text{-}1)$$

$$(1+\lambda_\xi^+\frac{\Delta t}{\Delta\xi}+\lambda_\xi^-\frac{\Delta t}{\Delta\xi}+\lambda_\eta^+\frac{\Delta t}{\Delta\eta}+\lambda_\eta^-\frac{\Delta t}{\Delta\eta})\delta U_{i,j}^{n+1}=\Delta U_{i,j}^{n}+\frac{\Delta t}{\Delta\xi}\lambda_\xi^+\delta U_{i-1,j}^{n+1}+\frac{\Delta t}{\Delta\xi}\lambda_\xi^-\delta U_{i+1,j}^{n+1}$$
$$+\frac{\Delta t}{\Delta\eta}\lambda_\eta^+\delta U_{i,j-1}^{n+1}+\frac{\Delta t}{\Delta\eta}\lambda_\xi^-\delta U_{i,j+1}^{n+1} \qquad (11\text{-}2)$$

It is important to note that, to solve a viscous flow, the explicit step $\Delta U_{i,j}^{n}$ must be differenced with second-order accuracy in order to avoid the numerical viscosity smearing of physical nature, thus we adopt:

∇_x = backward operator = $0.5(3u_j - 4u_{j-1} + u_{j-2})$ and,

Δ_x = forward operator = $0.5(-3u_j + 4u_{j+1} - u_{j+2})$.

Solving method for the implicit step

Figure 1 shows the grid distribution in the computational domain. The grid points are arranged from 1 to II along ξ direction, and from 1 to JJ along η direction. In order to solve the implicit step, equations (10-2) and (11-2) are rearranged in the following manner:

$$-\frac{\Delta t}{\Delta\eta}(\lambda_\eta^+)_{i,j}^{n}\delta U_{i,j-1}^{n+1}+[1+(\lambda_\xi^+)_{i,j}^{n}\frac{\Delta t}{\Delta\xi}+(\lambda_\xi^-)_{i,j}^{n}\frac{\Delta t}{\Delta\xi}+(\lambda_\eta^+)_{i,j}^{n}\frac{\Delta t}{\Delta\eta}+(\lambda_\eta^-)_{i,j}^{n}\frac{\Delta t}{\Delta\eta}]\delta U_{i,j}^{n+1}$$
$$-\frac{\Delta t}{\Delta\eta}(\lambda_\xi^-)_{i,j}^{n}\delta U_{i,j+1}^{n+1}=\Delta U_{i,j}^{n}+\frac{\Delta t}{\Delta\xi}(\lambda_\xi^+)_{i,j}^{n}\delta U_{i-1,j}^{n+1}+\frac{\Delta t}{\Delta\xi}(\lambda_\xi^-)_{i,j}^{n}\delta U_{i+1,j}^{n} \qquad (12)$$

The above equations can be solved easily by the Thomas algorithm[8]. Calculation begins with I = 1 station until I = II along ξ direction. At each I station, $\delta U_{i-1,j}^{n+1}$ term is just obtained and $\delta U_{i+1,j}^{n}$ is available with the value of the last time step, so the right hand side of equation (12) is all known. In this way, the unknown, $\delta U_{i,j-1}^{n+1}$, $\delta U_{i,j}^{n+1}$ and $\delta U_{i,j+1}^{n+1}$ can be obtained directly by the Thomas algorithm along η direction. Hence, an approximate factorization and

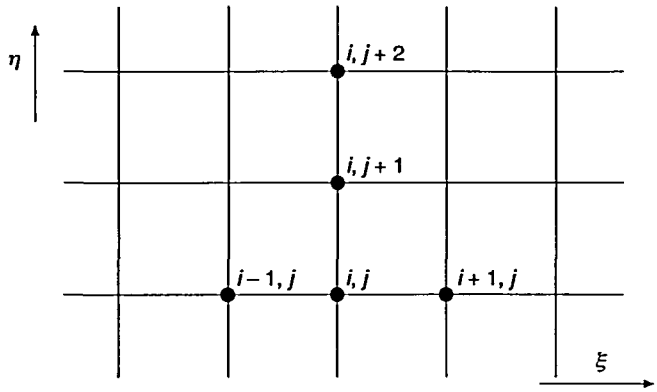

Figure 1 Grid distribution in computational domain

coefficient block-diagonal system of equations can be avoided successfully in solving equation (12).

Implicit boundary conditions

It is known from equation (12) that the implicit flux vector-splitting scheme consists of an explicit part $\Delta U^n_{i,j}$ and an implicit part $\delta U_{i,j}$. We propose $\delta U|_{Bound} = 0$ for the inlet, outlet and solid implicit boundary conditions. For the steady state calculation, when it approaches a convergent solution, $\partial U/\partial t$ will tend towards zero, i.e. $\delta U \to 0$. Therefore, at least in theory, this hypothesis is correct. For the periodical boundary condition that exists in the cascade calculation, the more realistic approach is to let $\delta U_{i,1} = \delta U_{i,JJ}$.

Stability analysis

The 2D Navier-Stokes equations in flux vector-splitting form (7) can be written as:

$$\frac{\partial U}{\partial t} + A^+\frac{\partial U}{\partial \xi} + A^-\frac{\partial U}{\partial \xi} + B^+\frac{\partial U}{\partial \eta} + B^-\frac{\partial U}{\partial \eta} = \frac{1}{\mathrm{Re}}\left(M_\xi\frac{\partial^2 U}{\partial \xi^2} + M_\eta\frac{\partial^2 U}{\partial \xi \partial \eta} + N_\xi\frac{\partial^2 U}{\partial \xi \partial \eta} + N_\eta\frac{\partial^2 U}{\partial \eta^2}\right) \tag{13}$$

where $A^\pm$, $B^\pm$, M_ξ, M_η, N_ξ and N_η are all matrices with:

$$A^+ = \frac{\partial F^+}{\partial U},\ A^- = \frac{\partial F^-}{\partial U},\ B^+ = \frac{\partial G^+}{\partial U},\ B^- = \frac{\partial G^-}{\partial U},\ M_\xi = \frac{\partial Q}{\partial(\frac{\partial U}{\partial \xi})},\ M_\eta = \frac{\partial Q}{\partial(\frac{\partial U}{\partial \eta})},$$

$$N_\xi = \frac{\partial R}{\partial(\frac{\partial U}{\partial \xi})} \text{ and } N_\eta = \frac{\partial R}{\partial(\frac{\partial U}{\partial \eta})}.$$

According to Liu's[12] 1D model equations and MacCormack-81 scheme's[2] stability conditions together with the characteristic theory of equations, we propose the following stability conditions for the current implicit scheme (12):

$$\lambda_\xi^+ = \max\{\rho(A^+) + \frac{2}{\mathrm{Re}\Delta\xi}[\rho(M_\xi)+\rho(M_\eta)] - \frac{\Delta\xi}{c\Delta t}, 0\}$$

$$\lambda_\xi^- = \max\{\rho(A^-) + \frac{2}{\mathrm{Re}\Delta\xi}[\rho(M_\xi)+\rho(M_\eta)] - \frac{\Delta\xi}{c\Delta t}, 0\}$$

$$\lambda_\eta^+ = \max\{\rho(B^+) + \frac{2}{\mathrm{Re}\Delta\eta}[\rho(N_\xi)+\rho(N_\eta)] - \frac{\Delta\eta}{c\Delta t}, 0\}$$

$$\lambda_\eta^- = \max\{\rho(B^-) + \frac{2}{\mathrm{Re}\Delta\eta}[\rho(N_\xi)+\rho(N_\eta)] - \frac{\Delta\eta}{c\Delta t}, 0\} \qquad (14\text{-}1)$$

where $\rho(A^\pm)$, $\rho(B^\pm)$, $\rho(M_\xi)$, $\rho(M_\eta)$, $\rho(N_\xi)$ and $\rho(N_\eta)$ are the spectral radii of the matrices $A^\pm$, $B^\pm$, M_ξ, M_η, N_ξ and N_η respectively. By solving these spectral radii, and putting them back into equation (14-1), the stability conditions can be obtained as follows:

$$\lambda_\xi^+ = \max\{|\tilde{U} + a\sqrt{\xi_x^2+\xi_y^2}| + \frac{2\omega}{\rho\Delta\xi}(\xi_x^2+\xi_y^2) - \frac{\Delta\xi}{c\Delta t}, 0\}$$

If $\tilde{U} - a\sqrt{\xi_x^2+\xi_y^2} < 0$, then:

$$\lambda_\xi^- = \max\{|\tilde{U} - a\sqrt{\xi_x^2+\xi_y^2}| + \frac{2\omega}{\rho\Delta\xi}(\xi_x^2+\xi_y^2) - \frac{\Delta\xi}{c\Delta t}, 0\};$$

else, $\lambda_\xi^- = 0$.

$$\lambda_\eta^+ = \max\{|\tilde{V} + a\sqrt{\eta_x^2+\eta_y^2}| + \frac{2\omega}{\rho\Delta\eta}(\eta_x^2+\eta_y^2) - \frac{\Delta\eta}{c\Delta t}, 0\}$$

If $\tilde{V} - a\sqrt{\eta_x^2+\eta_y^2} < 0$, then:

$$\lambda_\eta^- = \max\{|\tilde{V} - a\sqrt{\eta_x^2+\eta_y^2}| + \frac{2\omega}{\rho\Delta\eta}(\eta_x^2+\eta_y^2) - \frac{\Delta\eta}{c\Delta t}, 0\}$$

else, $\lambda_\eta^- = 0$. (14-2)

where $\omega = \max\left(\frac{\mu}{\mathrm{Re}}, \frac{\mu' + 2\mu}{\mathrm{Re}}, \frac{\mu\gamma}{\mathrm{Pr}\,\mathrm{Re}}\right)$ a is speed of sound, μ' is the second coefficient of μ, and $c = 2$.

Likewise, we can also obtain the stability conditions for an inviscid flow with $(2\omega|\rho)$ terms = 0. In principle, when λs are chosen from equation (12) or (13), the implicit method (9) or (8) can be granted as a stable scheme at any time step. Therefore, we could say that the schemes (8) and (9) are unconditionally stable from this point of view.

Time-step length

We choose the time-step length according to the following CFL number definition:

$$\Delta t = \min\{\Delta t_\xi, \Delta t_\eta\} \tag{15}$$

For inviscid flow:

$$\Delta t_\xi \le \frac{CFL \bullet \Delta\xi}{\max\limits_{i,j} \{|\tilde{U}| + a\sqrt{\xi_x^2 + \xi_y^2}\}}$$

$$\Delta t_\eta \le \frac{CFL \bullet \Delta\eta}{\max\limits_{i,j} \{|\tilde{V}| + a\sqrt{\eta_x^2 + \eta_y^2}\}}$$

For viscous flow:

$$\Delta t_\xi \le \frac{CFL \bullet \Delta\xi}{\max\limits_{i,j} \{|\tilde{U}| + a\sqrt{\xi_x^2 + \xi_y^2} + \frac{2\gamma}{\rho\Delta\xi}(\xi_x^2 + \xi_y^2)\}}$$

$$\Delta t_\eta \le \frac{CFL \bullet \Delta\eta}{\max\limits_{i,j} \{|\tilde{V}| + a\sqrt{\eta_x^2 + \eta_y^2} + \frac{2\gamma}{\rho\Delta\eta}(\eta_x^2 + \eta_y^2)\}}$$

It is obvious that when the CFL number is smaller than or equal to 1.0, Δt is the time-step length for an explicit scheme, and $\lambda_\xi^\pm$ and $\lambda_\eta^\pm$ of the whole field will pose to zero automatically. Therefore, the implicit scheme will reduce to the explicit scheme in this case.

In the current calculation, the CFL number for the implicit scheme is chosen to be about 30. But for a specific problem, it is restricted by many factors. For example, when the grid distribution is uniform, the CFL number can be even higher, otherwise it can only be given to be around eight for complex geometries and grid generation.

Convergence criteria

There are various methods to check whether the result has converged to the steady state solution. In the present work, the following two convergence criteria are used:

$$1)\ \left(\frac{\Delta U}{\Delta t}\right)_{max} \le \varepsilon_n \ ; \quad 2)\ \left(\frac{\Delta\varphi}{\varphi}\right)_{max} \le \varepsilon_\varphi$$

where U is the same term as used in schemes (11) and (12), ΔU is the difference between the two iteration steps and φ is any other gasdynamics parameter, $(\Delta\varphi/\varphi)_{max}$ is the maximum relative difference of that gasdynamics parameter at any grid point. Note that the values of ε_n and ε_φ are both assigned as 1×10^{-4}.

COMPUTATIONAL RESULTS AND SAMPLE APPLICATIONS

Based on the efficient flux vector-splitting implicit scheme, the algebraic H-grid generator and Baldwin-Lomax turbulent model[13], a software package for solving the 2D Euler and time-averaged Navier-Stokes equations is developed.

Study of the typical convergence histories with different CFL numbers

Typical convergence histories with both inviscid and viscous flows are presented in Figures 2 and 3 for the computation of convergence-divergence nozzle flows with their grid distributions of (35 × 15) and (41 × 25) respectively where the operating mode of supersonic flows at exit are being considered.

Figure 2 reveals the convergence history with CFL = 0.8, 5, 10, 25 and 100 for inviscid flow. From this figure, we can see that the convergence rate is improved significantly when larger CFL numbers are used. For example, the norm residual reduces four orders of magnitude with 300 iteration time steps for CFL = 25, as compared to 1,000 iteration steps in the case of CFL = 5 to reduce the same order of magnitude. Also, in the case of CFL = 0.8, which means the implicit scheme reduces to the explicit scheme, it only drops 1.5 orders of magnitude with 2,000 iteration steps. However, there is no obvious effect on improving the convergence rate by continually increasing the CFL number.

Figure 3 indicates the convergence history with CFL = 0.8, 2, 5, 8, 10 and 12 for viscous flow. Because the flux vectors associated with viscous terms Q and R are not split into the upwind forms (central differencing is used here), as highlighted in the section on construction of an efficient flux vector-splitting implicit scheme, the convergence ability is influenced and thus the CFL number cannot be as large as in the inviscid flow calculation. Nevertheless, the convergence rates are improved significantly when larger CFL numbers are used.

In general, it is better to choose a CFL number in the range of 20 to 30 for inviscid calculation and between 5 and 10 for viscous flow computation when using the present efficient flux vector-splitting implicit scheme. In such a case, only about 300 to 500 iteration time steps are needed to obtain the satisfactory convergent result for the inviscid calculation and about 600 iteration time steps for viscous prediction. The code runs at about 1.042×10^{-4} seconds per point per time step for inviscid flow and about 1.902×10^{-4} seconds per point per time step for viscous flow on a Vax-9000 machine.

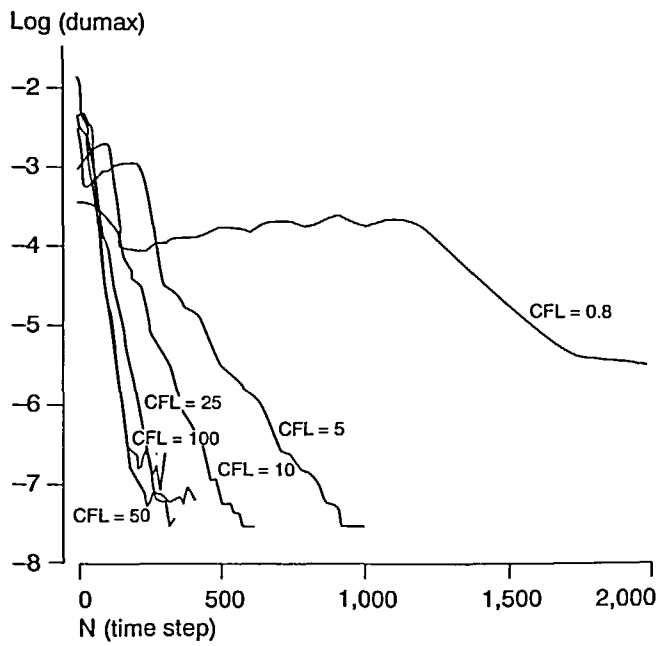

Figure 2 Typical convergence history with different CFL numbers (inviscid flow – C-D nozzle)

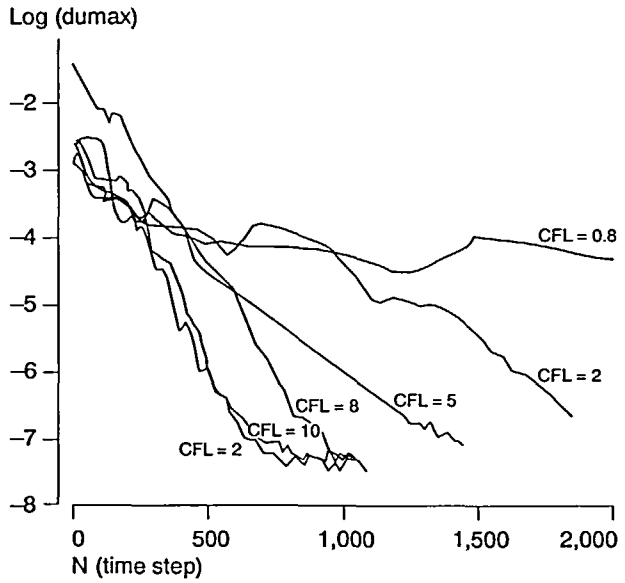

Figure 3 Typical convergence history with different CFL numbers (viscous flow – C-D nozzle)

Convergence-divergence nozzle flow

In the first example, both the inviscid and viscous computations for two operating conditions with exit isentropic Mach numbers (M_{2is}) of 1.6 and 0.6 are carried out on the nozzle domain.

First, the operating mode of supersonic flow at exit is considered. Figure 4 shows the comparison of the inviscid and viscous predicted surface pressure distributions with experimental data taken from Zheng[14]. It is found that both inviscid and viscous numerical solutions agree

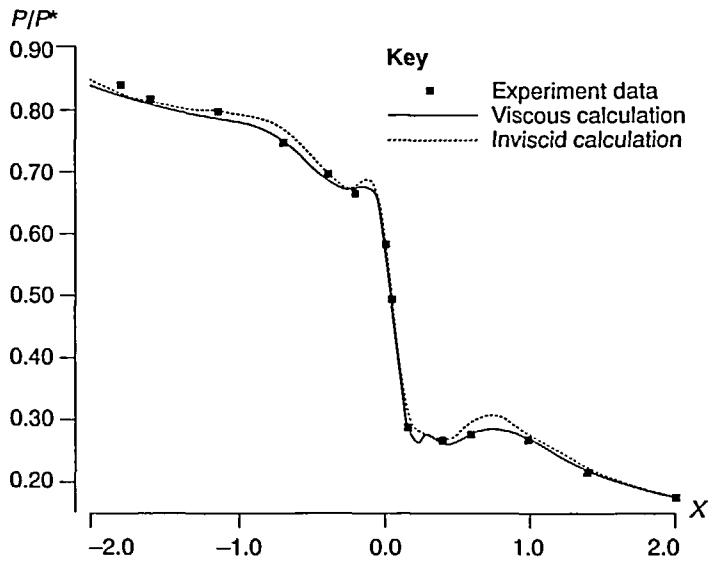

Figure 4 Surface static pressure distributions of nozzle flows (1st mode)

closely with the measured result, in which the viscous prediction has a better agreement. Second, the operating mode of having a shock wave is computed. Figures 5 and 6 present the Mach number contours obtained from the inviscid and viscous calculations respectively. From these contours, both the changes of Mach number distribution when shock wave appears and the differences in the velocity distribution for inviscid and viscous flow predictions can be clearly discerned. As before, *Figure 7 shows the comparison of the inviscid and viscous predicted surface pressure distributions* with experimental data taken from Zheng[14], and both inviscid and viscous numerical solutions agree very well against the measured result. Here, the y^+ value of the first node next to the wall is 3.0 for the Navier-Stokes case.

In the above calculation, only about 300 time steps with CFL = 30 and about 500 time steps with CFL = 10 are required for the inviscid and viscous calculations respectively to obtain satisfactory results.

Transonic turbine cascade

The second test case consists of the inviscid and viscous calculations through a transonic turbine cascade. The code used a simple H-grid system with (41 × 25) points for both viscous and inviscid

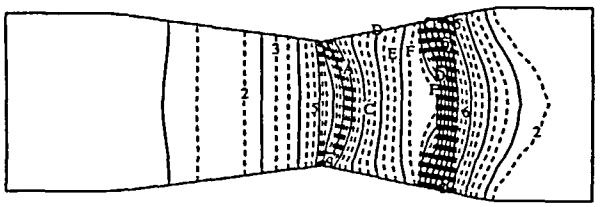

Level	MACH
F	1.54827
E	1.47521
D	1.40214
C	1.32908
B	1.25602
A	1.18296
9	1.10989
8	1.03683
7	0.963769
6	0.890706
5	0.817644
4	0.744581
3	0.671519
2	0.598456
1	0.488862

Figure 5 Mach number contours (inviscid – 2nd mode)

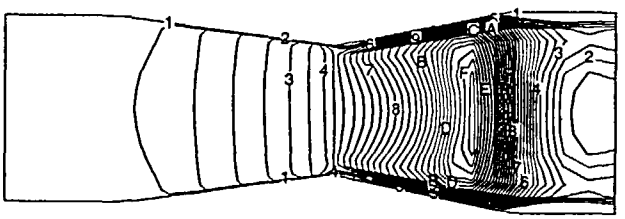

Level	MACH
F	1.90
E	1.79
D	1.69
C	1.59
B	1.49
A	1.38
9	1.28
8	1.18
7	1.08
6	0.97
5	0.87
4	0.77
3	0.67
2	0.56
1	0.46

Figure 6 Mach number contours (viscous – 2nd mode)

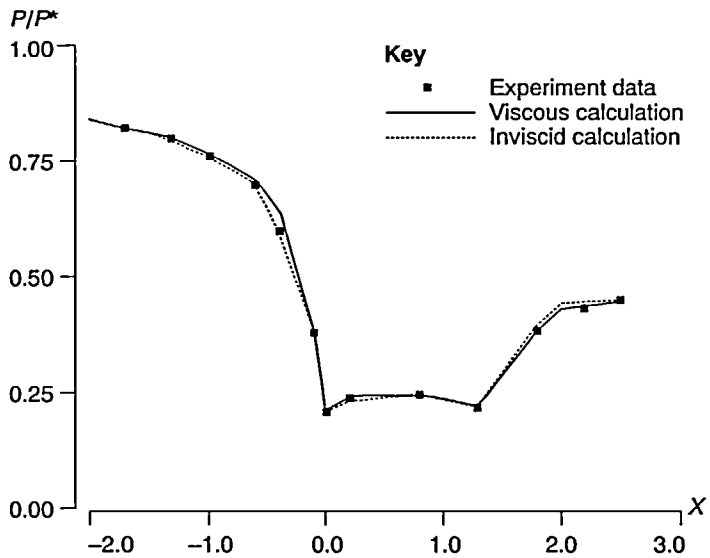

Figure 7 Surface static pressure distributions of nozzle flows (2nd mode)

flows as shown in Figure 8, where the y^+ value for the first node next to the blade surface is 2.0. The flow conditions are as follows:

Inlet stagnation pressure $P_0^* = 199{,}555\ N/m^2$

Inlet stagnation temperature $T_0^* = 288°\ K$

Outlet static pressure $P_b = 102{,}318.3\ N/m^2$

Inlet flow angle $\alpha = -21.2°$

Cascade pitch $t = 0.09163m$

Comparisons between the inviscid and viscous calculations are conducted. Figure 9 presents the surface pressure distributions. The triangle and square symbols indicate the measured data obtained from Zhang[15]. The short and long dash lines illustrate the current inviscid prediction on suction and pressure surfaces respectively while the solid and dash-dot-dot lines represent viscous prediction results on suction and pressure walls. The shock wave is captured accurately in both cases as compared to the experimental result except a slightly higher prediction occurs in the suction surface pressure distribution with the inviscid flow calculation (due to zero blade boundary layer as expected). Finally, Figure 10 illustrates the Mach contour distributions for the inviscid and viscous flow predictions; their differences can be clearly discerned. In the above calculations, about 600 and 900 iterate time steps are needed for inviscid and viscous flows with CFL = 18 and 9 respectively.

CONCLUSIONS

A one-step efficient flux vector-splitting implicit scheme suitable for both inviscid and viscous 2D flow calculations has been developed successfully. It has the following special advantageous characteristics:

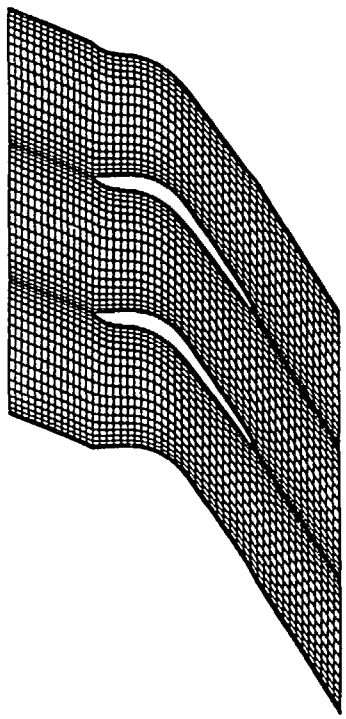

Figure 8 Grid used for transonic turbine flows (inviscid and viscous)

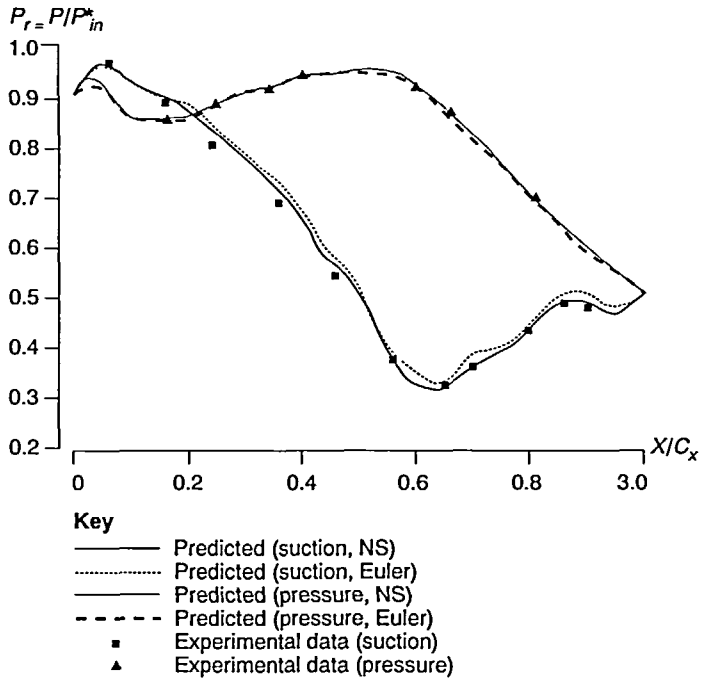

Figure 9 Surface static pressure distributions of transonic turbine cascades

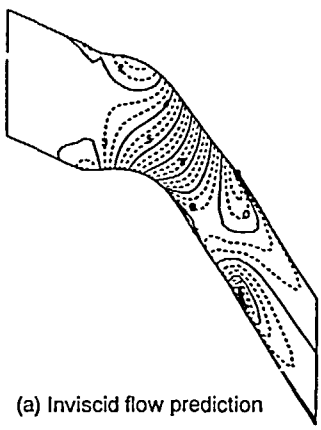

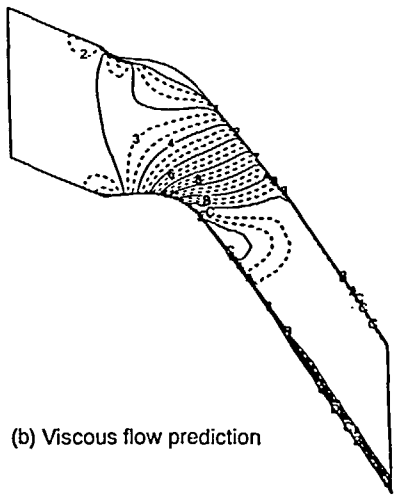

Figure 10 Mach contour distributions (inviscid and viscous)

(1) A significant improvement in computational efficiency is achieved as compared to the well-known Beam and Warming[1] and Steger[16] implicit factored schemes because it has an advantage in the formulating of higher-order numerical implicit terms.

(2) The weakness of no superior in the main diagonal of coefficient matrix in conventional approximate factorization method is avoided and the solving procedure is improved.

(3) Spectral radii technique is used to replace the coefficient matrix calculation, hence the 3×3 systems of equations are being transformed to the three scalar equations in the current 2D work, where comparatively fewer computational efforts are needed.

(4) No approximate factorization occurs in the time-marching process, so there is no numerical error caused by an approximate factorization, and it helps to increase the CFL number for calculation.

(5) It is a one-step scheme which aims to improve the convergent ability, especially for large time-step computations, as it can converge to the numerical solution with zero output of computer's error in principle.

(6) The flux vector-splitting implicit scheme is an upwind scheme, the flux-vector is split according to the physical characteristics and corresponding difference schemes are adopted to restrain the numerical errors. Thus it is a stable scheme without the need to add any artificial viscosity and simplifies the calculation.

Finally, the concepts involved in the construction of an implicit scheme with an exact factorization and avoiding of the coefficient block-diagonal system of equations, together with their successful applications, provide future prospects for further development in 3D problems.

REFERENCES

1 Beam, R.M. and Warming, R.F., An implicit finite-difference algorithm for hyperbolic systems in conservation-law form, *Journal of Computational Physics*, Vol. 22, 87-110 (1976)
2 MacCormack, R.W., A numerical method for solving the eqs of comp. viscous flow, *AIAA Paper 81-0110* (1981)
3 Von Lavante, E. and Lyer, V., Simplified implicit block-bidiagonal finite difference method for solving the Navier-Stokes equations, *AIAA Journal*, Vol. 23 No. 7 (1985)
4 Dawes, W.N., Development of a 3D Navier-Stokes solver for application to all types of turbomachinery, ASME Paper No. 88-GT-70 (1988)
5 Jameson, A., Successes & challenges in computational aerodynamics, *Proc. of AIAA 8th CFD Conf.* Honolulu, HI, 1-35 (1987)
6 Sankar, N.L., Malone, J.B. and Tassa, Y., An implicit conservative algorithm for steady and unsteady three-dimensional potential flows, *AIAA Paper 81-1016* (1981)
7 Ames, W.F., *Numerical Methods for Partial Differential Equations,* 2nd ed., Academic, New York (1977)
8 Anderson D.A., Tannehill, J.C. and Pletcher, R.H., *Computational Fluid Mechanics and Heat Transfer*, Hemisphere Publishing Corporation, New York (1984)
9 Hedstrom, G.W., Nonreflecting boundary conditions for nonlinear hyperbolic systems, *J. of Comp. Physics*, Vol. 32 (1979)
10 Chakravarthy, S.R., Anderson, D.A. and Salas, M.D., The split coefficient matrix method for hyperbolic systems of gasdynamics equations, *AIAA Paper 80-0268* (1980)
11 Moretti, G., An old integration scheme for compressible flows revisited, refurbished and put to work, *Computational Fluids,* Vol. 7, 191 (1979)
12 Liu B., Axial vaneless nozzle turbine stage – principle, design and calculation, PhD thesis Xi'an Jiaotong University, People's Republic of China (1989)
13 Baldwin, B.S. and Lomax, H., Thin layer approximation and algebraic model for separated turbulent flows, *AIAA Paper 78-257 (1978)*
14 Zheng X., Transonic flow calculation for 2D nozzle, *J. of Aero., P.R.China*, Vol. 7 No. 4 (1989)
15 Zhang Y., Some problem about transonic flow calculation using the time-related method, *J. of Engg. Thermal Physics,* People's Republic of China, Vol. 1 No. 4 (1980)
16 Steger, J.L., Coefficient matrices for implicit finite difference solution of the inviscid fluid conservation law equations, *Computer Methods in Applied Mechanics and Engineering*, Vol. 13, 175 (1978)